Quasi-elastic light scattering in betaine calcium chloride dihydrate (BCCD)

1999 J. Phys.: Condens. Matter 11 10459

(http://iopscience.iop.org/0953-8984/11/50/334)

J. Phys.: Condens. Matter **11** (1999) 10459–10473. Printed in the UK PII: S0953-8984(99)01014-0

Quasi-elastic light scattering in betaine calcium chloride dihydrate (BCCD)*

M Schmitt-Lewen† and G Schaack

Physikalisches Institut der Universität Würzburg, Am Hubland, D-97074 Würzburg, Federal Republic of Germany

Received 18 January 1999, in final form 5 July 1999

Abstract. We report measurements of the temperature (40 K $\leqslant T \leqslant$ 200 K) and polarization ($z(yy)x$, $z(xz)x$) dependence of the integrated intensities of quasi-elastically scattered laser light ($\lambda = 514.5$ nm) in a wavenumber interval of 0 ± 3 cm^{-1} around the Rayleigh line at the different phase transitions in single crystals of BCCD. Large anomalies (central peaks) are observed at the transitions into the ferroelectric, the various commensurate (c, c$'$), and the incommensurate phases. The widths of the anomalies on the temperature scale are large in the regions of quasi-harmonic modulation of the structure, but narrow and distinct in the region of square-wave modulation in the solitonic phase of BCCD, where also unusual shapes on the T-axis are observed. The scattering phenomena at low temperatures are interpreted hypothetically as due to fluctuations caused by the formation or rearrangement of domain walls (solitons) in the lattice near the transitions between commensurate phases and by the variation in soliton density. The c $\leftrightarrow$ c$'$ transitions are of the order–disorder type.

1. Introduction

The unusually large number of commensurately (c) and incommensurately (ic) modulated phases observed in betaine calcium chloride dihydrate ($(CH_3)_3 \cdot NCH_2COO \cdot CaCl_2 \cdot 2H_2O$ (BCCD), $Pnma$ (D_{2h}^{16}), $Z = 4$ in the n phase at 300 K) has given this material a prominent position among the spontaneously modulated crystal structures known of today [1]. The information available at present on BCCD has been reviewed recently [2]. BCCD displays a 'devil's staircase' behaviour of its modulation wavevector $\boldsymbol{q} = \delta(T)\boldsymbol{c}^*$, below the transition into an ic phase at $T_i = 164$ K ($\delta(T_i) = 0.319$). The devil's staircase is incomplete in the region $T_i \geqslant T \geqslant 115$ K with a sequence of alternating ic and c phases. It is harmless below the onset of the $\delta = \frac{1}{4}$ phase at 115 K ($=T_{L_2}$), which is followed by the sequence of $\frac{1}{5}, \frac{2}{9}, \frac{1}{6}, \ldots$ phases, and down to the homogeneously polarized ferroelectric (fe) phase $\delta = 0$ starting at $T_0 = 46$ K. The spontaneous polarization in the fe phase is along the y-direction of the crystal, while most of the c phases also display a spontaneous polarization P_s according to the following symmetry-based rule: $\boldsymbol{P}_s \parallel \boldsymbol{y}$ if $\delta =$ even/odd, $\boldsymbol{P}_s \parallel \boldsymbol{x}$ if $\delta =$ odd/even, $P_s = 0$ if $\delta =$ odd/odd; [3, 4]. All three lattice constants a, b, c in the n phase are close to 1 nm [2].

A theoretical interpretation of the phase diagram has been achieved on the basis of the semi-microscopic Ising pseudo-spin models [5], either the simple ANNNI model [6] (axial next-nearest-neighbour Ising) or the more involved DIS model [7] (double Ising-spin), which is a pseudo-spin modification of a symmetry-adapted local mode model which is well suited

* Dedicated to the memory of H-G Unruh.

† Now at: Heidelberger Druckmaschinen AG, 69116 Heidelberg, Germany.

to BCCD. In this DIS model the pseudo-spin components are the signs of the displacement coordinates of relevant atoms or molecular groups which are involved in the transition. Another model, based on such symmetry-adapted variables, has also been developed and specifically applied to BCCD in reference [8]. The phenomenological Landau approach has been adapted to the case of BCCD in references [9] and [10].

BCCD has been considered for a long time as belonging to the group of class-II systems [11, 12] of ic modulated materials, as its phase diagram displays a Lifshitz point [13] and the low-temperature phase is unmodulated ($\delta = 0$). Moreover, the effects of solitonic (non-harmonic) modulation just above the lock-in transitions $T_{L_1} = 128$ K into the $\delta = \frac{2}{7}$ phase and $T_{L_2} = 115$ K into the $\delta = \frac{1}{4}$ phase were found to be small [14], as expected. However, this view very probably has to be revised, because of recent experimental results. Hernandez, Quilichini and co-workers [15] have studied again the structure of deuterated BCCD in its $\delta = \frac{1}{4}$ phase and performed a completely new structure determination of the $\delta = \frac{1}{5}$ phase by neutron diffraction, thus avoiding the uncontrollable effects of radiation damage by x-rays of the subtle structures of the modulated phases [2]. It was observed that the modulation in both phases, as demonstrated by the atomic modulation functions, is close to square wave, i.e. strongly anharmonic; this is in contrast to the case for earlier x-ray investigations, which indicated a quasi-harmonic modulation down to T_0 [16]. This result is supported by dielectric studies of BCCD under the application of a strong electric field along the y-direction [17]. The findings of this investigation can only be understood assuming the existence of domain walls (solitons), interacting repulsively with each other [17], which separate the microdomains of parallel Ising pseudo-spins in the modulated phases from the neighbouring microdomains with opposite pseudo-spin orientation. These domains have a width w of half the modulation wavelength $\lambda_{mod} = c/\delta$ for the $\delta = 1/m$ phases, (m integer). The phases $\delta = 2/m'$ (m' integer and odd) display domain widths w' alternating between $w'_{1,2} = (c/2)(m' \pm 1)$. These phases have a very narrow range of stability on the T-axis.

In these domain walls, which have a finite width of about one lattice constant ($\approx$1 nm) [17], and thus differ qualitatively from the usual domain walls in the fe phase of a ferroelectric material [18], the Ising pseudo-spins are randomly oriented, i.e. the domain walls are rough, thus storing all the entropy produced at T_0 and at higher c $\to$ c$'$ phase transitions, as becomes evident from specific heat measurements at these transitions [19]. Here the relation was established that the entropy $\Delta S_{c,c'}$ produced at the phase transition c $\leftrightarrow$ c$'$ is proportional to $\Delta\delta_{c,c'}$ or to $\Delta\bar{n}_{c,c'}$, the difference in soliton density between two adjacent phases. Further experimental support for the existence of these domain walls is provided by the recent observation [20] that the jumps of the tensile strain at the c $\leftrightarrow$ c$'$ phase transitions in BCCD, as evidenced by the thermal expansion in the modulation direction and observed by Freitag and Unruh [14], are proportional to the difference $\Delta\delta_{c,c'}$ of the wavevectors of the adjacent c phases, i.e. again to $\Delta\bar{n}_{c,c'}$. Bak already postulated the existence of such a relation in anharmonically modulated structures, a long time ago [21].

All of this gives strong evidence that in the interval 46 K $\leqslant T \leqslant$ 115 K a solitonic phase exists in BCCD where the solitons can be considered as interacting quasi-particles, forming a one-dimensional soliton lattice, i.e. the solitons extend in the x–y plane with the normal of the wave fronts along the direction of the modulation wavevector $\boldsymbol{q}_z$. The soliton density $\bar{n}(T) = \delta(T)$ [2] can also be considered as a second (or alternative) order parameter, which is, of course, coupled to the primary order parameter of symmetry Λ_3 [3], the amplitude of the structural distortion, to produce the observed phase diagram. In a Landau expansion of the free energy with respect to the first order parameter [9, 10], where all symmetry-allowed terms are included, the contributions due to the interacting solitons [22] are of course already considered implicitly. The observation of electric-field-induced structural phase transitions in the soliton lattice of BCCD [17], which have recently been verified by means of neutron diffraction [23], gives additional support to this hypothesis. BCCD can be viewed in this temperature range as a spontaneously formed nanostructure with a temperature- and field-dependent structural width and with the solitons as interfaces.

This hypothesis gives strong motivation to emphasize research on the hitherto rather neglected phase transition at T_0. This appears to be a truly unique transition from an almost saturated proper fe phase ($\delta = 0$) at low T to a sequence of similarly saturated layers with alternating directions of polarization separated by interfaces of finite width. Below T_0, BCCD can be considered as a three-dimensional Ising system, with all pseudo-spins pointing in one direction (particles in one minimum of a double-minimum, single-particle potential) in the fe phase. Above T_0, in the $\delta = 1/m$ phases, δ^{-1} layers of pseudo-spins point in one direction, the following δ^{-1} pseudo-spin layers point in the opposite direction, etc. The lattice becomes unstable against the creation of domain walls, which destroys the long-range order, i.e. lowers the translational symmetry. As the phase transitions c $\leftrightarrow$ c$'$ $\leftrightarrow$ fe are close to second order [2], they are accompanied by strong fluctuations of n, i.e. of the entropy density. The mobile domain walls which exist in the fe phase above their freezing temperatures [2, 24] in a polydomain crystal do not contribute to the instability, as the transition entropy generated at T_0 for the transition fe $\rightarrow$ $c_{1/6}$ is the same at low fields in the polydomain crystal as at high electric fields $\|\boldsymbol{y}$ in the single-domain case [17]. One immediately realizes that for the transition at T_0 the familiar concept of a quasi-harmonic soft phonon or relaxational mode triggering the transition as in a weakly anharmonic lattice has to fail. Other, strongly non-linear excitations have to be considered in addition. The possible existence of another 'Goldstone mode' at T_0 is an interesting question.

It should be remembered that solitons in class-I systems (e.g. in A_2BX_4 materials) only occur above the lock-in temperature T_L, where the transition into the c phase takes place. These solitons usually display a phase shift of $\pi/3$ and annihilate at T_L in a stripple process (see e.g. [25]), where a stripple is built up from domains of the reference c phase. The domains of the stripple are separated by discommensuration planes. In the Ising system BCCD, however, this shift amounts to π and the solitons annihilate at T_0 which in this respect corresponds to T_L in class-I systems.

The rearrangement of soliton positions with respect to the underlying lattice and the soliton dynamics at the c $\rightarrow$ c$'$ phase transitions should be observable both in light and in neutron scattering experiments [26]. As a first step in this direction, we report here observations of scattering of laser light near the Rayleigh line at various phase transitions in the temperature range of the modulated phases of BCCD. These measurements should be considered as preliminary. They represent, on the other hand, interesting results on this unconventional system, and it is hoped that they will stimulate more elaborate and detailed experiments involving variation of temperature, pressure, electric field, and impurity concentration and, in particular, high spectroscopic resolution.

2. Experimental results

For the experiment we used a standard Raman instrument (a DILOR triple monochromator, $f = 50$ cm, in the additive (high-resolution) mode) in 90° geometry at the fixed wavelength of the exciting Ar^+-ion laser $\lambda = 514.5$ nm, using a photomultiplier as detector and photocounting electronics for the data acquisition with an integration time of 10 s. The slit widths were selected to provide a spectral window of 0 ± 3 cm^{-1} for the observation of the quasi-Rayleigh scattering. The sample, carefully selected for its optical homogeneity and orientation, was attached to the cold finger of a liquid-helium evaporation cryostat with automatic temperature control, both by sample heating and regulation of the evaporation rate. A Pt resistance thermometer close to the sample was used to monitor the temperature. The sample had to be kept in vacuum. Attempts to use a He exchange gas for the reduction of the temperature difference between the sample and cold finger were unsuccessful because of the disturbance of the laser beam by thermal convection. A temperature scan rate of ± 0.05 K s^{-1} was chosen as a compromise between the requirements for an optimum signal-to-noise ratio on the one hand and the detrimental effects of the long-term thermal instability of the entire instrumentation on the other. We have evaluated only the spectra taken at a positive temperature gradient; the spectra with the negative gradient display stronger noise for otherwise similar appearance. The stability requirements for this type of experiment are far more stringent than for an ordinary inelastic light scattering set-up. The laser power entering the cryostat was 2 mW in $z(yy)x$ polarization, 13 mW in $z(xz)x$ polarization†, giving rise to temperature shifts ($\approx$6 K) between the observed anomalies and the known transition temperatures [2]. This was taken into account in figures 1 and 2 by shifting the temperature scales to achieve an acceptable agreement with the known values on average.

The results obtained are displayed in figures 1(a), 1(b), and 2. For ease of comparison, the well known dielectric function $\epsilon(y, T)$ (with the electric field in the direction of the spontaneous polarization) is also plotted in figure 1(a) [27]. $\epsilon(x, T)$ is not plotted, because it shows a single anomaly at $T_{L_2} = 115$ K and some minor peaks below that temperature, but a definite plateau-like minimum in the non-polar $\delta = \frac{1}{5}$ phase ($\epsilon_{1/5}(x, T) \approx 6.3$; $\epsilon_{1/6}(x, T) \approx 6.4$; $6.45 \leqslant \epsilon_{1/4}(x, T) \leqslant 28$). $\epsilon(z, T) =$ constant ($\approx$4) [27]. This minimum of ϵ or of the polarizability should also be encountered in the region of optical frequencies, as the infrared spectra of BCCD in the $\frac{1}{4}$, $\frac{1}{5}$, and $\frac{1}{6}$ phases (i.e. the contributions of ionic polarizabilities) do not differ drastically [28, 29].

The region around T_0 in the yy spectrum is reproduced for clarity on a larger T-scale in figure 2.

The following features in the two plots are clearly evident:

(1) The quasi-Rayleigh scattering in BCCD is strongly temperature dependent with at least six distinct anomalies of the intensity between T_i and T_0. All anomalies obey strict rules of polarization. The variation in integrated intensities amounts to less than one order of magnitude above the background level. Central-peak anomalies at c $\leftrightarrow$ c$'$ transitions are observed in those polarization directions which are distinguished as directions of the spontaneous polarization $\langle P_s \rangle$ and of its fluctuations δP_s for one of the c phases involved. The narrow peak at T_0 in the $z(yy)x$ spectrum receives its intensity from the polar (y) 0/1 phase; the asymmetric peaks in the $z(xz)x$ spectrum derive their strengths from the polar (x) phases $\frac{1}{4}$ and $\frac{1}{6}$, respectively. The spontaneous polarization in the 0/1 phase ($Pn2_1a$, C_{2v}^9) transforms according to A_1 of C_{2v}, which is correlated to A_g (yy) of D_{2h}, while the x-polarization transforms as B_1 of C_{2v}, corresponding to B_{2g} (xz) of D_{2h}. In general, central-peak scattering in BCCD can be observed in these Raman-active types having the symmetry of the prototype factor group, which are correlated with the irreducible representations transforming as the observed spontaneous polarization in the corresponding subgroups of the c phases of lower symmetry. Thus the polarization properties of central peaks in BCCD are governed by symmetry.

(2) The temperature interval investigated can be decomposed into at least two qualitatively different regimes: between T_i and T_{L_2}, where the $\delta = \frac{1}{4}$ phase is entered, the intensity anomalies are broad ($\approx$20 K fwhm) and approximately symmetric. Below T_{L_2} the

† The Porto notation $z(xz)x$ is used for the scattering geometry: the letters outside the brackets give the propagation directions of the incident (z) and the scattered (x) linearly polarized light; the bracketed letters are the respective polarization directions of the incident (x) and the scattered (z) radiation.

anomalies are narrow ($\leqslant$5 K fwhm) and the peaks are asymmetric with respect to the T-axis. This is clearly apparent for the two 'dispersion'-shaped peaks in the xz polarization which border the $\delta = \frac{1}{5}$ phase symmetrically. The extremely sharp peak at T_0 also displays an asymmetric shape (figure 2). The transition between the two regimes becomes evident in the xz polarization at $T = 115$ K, marked by a broad asymmetric peak with a steep slope at $T \leqslant 115$ K. The intensity minimum in the $\delta = \frac{1}{4}$ phase and the maximum in the $\frac{1}{5}$ phase are symmetric, indicating a stable state of the system here without fluctuations.

(3) The transition between the two regimes coincides with the onset of the square-wave modulation in the $\delta = \frac{1}{4}$ phase and with the T_S-anomaly [15, 17, 30, 31].

In the case of the $z(yy)x$ scattering geometry (polarized scattering), an increase of the intensity is observed with decreasing T, which has a maximum at T_i. This has to be attributed both to the quasi-condensation of a Raman-active A_g mode at T_i and the occurrence of an intrinsic central peak [32, 33], which is also observed in inelastic neutron scattering [34]. Below T_i the intensity goes through a relative minimum and displays another maximum at $\approx$140 K, which again is related to the low-frequency structure in the A_g Raman spectra in this temperature interval [32, 33]. While this structure has to be ascribed to the amplitudon mode [35], the phason is not Raman active here because the parent phase is centrosymmetric (D_{2h}); i.e. both modes, the amplitudon (g) and the phason (u), have a definite parity. The $\delta = \frac{2}{7}$ phase, which is prominent in the $\epsilon_y(T)$ dielectric function, produces a rather inconspicuous shoulder in the yy polarization. Throughout the region of the c phases the intensity is low; the polar $\delta = \frac{2}{9}$ and $\frac{2}{11}$ phases probably do not occur in our sample, or produce small effects, just above the noise level. The transition at T_0 into the fe phase, however, is most prominent, with $\approx$1 K fwhm. The peak is asymmetric; the modulus of the temperature gradient of the intensity is larger on the high-temperature side than on the low-temperature one. Such a behaviour is often encountered for critical scattering of light or neutrons by order–disorder phase transitions [37–40], where the low-gradient slope extends into the high-symmetry phase, which is the fe phase in our case. The steep slope descends into the 'ordered' phase, i.e. the solitonic $\delta = \frac{1}{6}$ phase.

The $z(xz)y$ polarization (depolarized scattering) demonstrates a considerably reduced cross section as compared to the polarized case and a continuous increase of the intensity with no anomaly at T_i, which is parallelled by the variation of the B_{2g} Raman spectra at low frequencies, and a sharp cut-off from an intensity maximum at the onset of the $\delta = \frac{1}{4}$ phase at T_{L_2}. This cut-off marks the low-temperature slope of a strong anomaly at 115 K. The non-polar $\delta = \frac{1}{5}$ phase is framed by two strongly asymmetric, dispersion-shaped anomalies with opposite phase shifts. The weak anomaly at T_0 may be due to a polarization leakage of the strong peak in the yy polarization.

Central peaks are only detected in the scattering geometries depicted in figure 1. Other geometries (xx, zz, (A_g), xy (B_{1g}) or zy (B_{3g})) do not display any intensity anomalies, as was also observed by Wilhelm and Unruh [33]. While the broad features in the plots above $\approx$115 K are mostly due to the quasi-condensation of soft modes, presumably with some unresolved contributions of coupling with low-lying relaxational modes [33], below this temperature the Raman spectra [32] are free from any harmonic excitations at very low frequencies. The lowest optical modes observed by inelastic neutron scattering at 35 K [40] are one B_{1g} and one B_{3g} mode near 30 cm^{-1} and one A_u mode, identical with the LA branch in the extended Brillouin zone, at 27 cm^{-1}.

Central peaks of the types described here have never been observed before in modulated structures where the modulation is known to be harmonic.

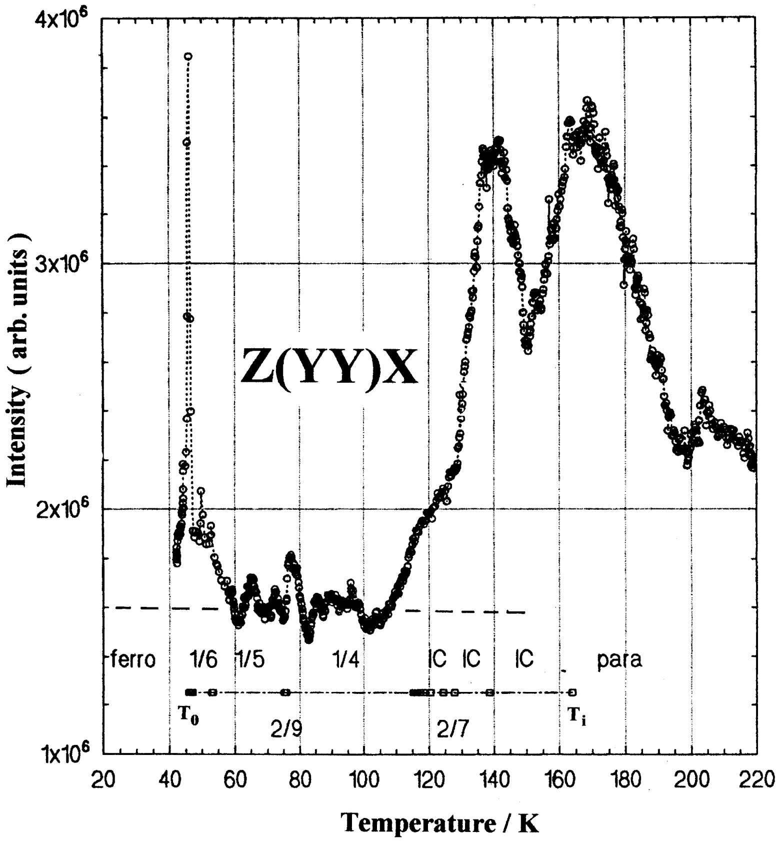

(a)

Figure 1. (a) The temperature dependence of the intensity of the Rayleigh scattering in $z(xz)x$ geometry for BCCD at ambient pressure (logarithmic scale), with $dT/dt > 0$. The sequence of ic and c phases has been given as well as the dielectric function (D.C.) $\epsilon_y(T)$ (above) for comparison. (b) $z(yy)x$ geometry; $dT/dt > 0$; linear scale. The horizontal dashed line gives the arbitrarily chosen background level for the plots in figure 2.

3. Discussion

Numerous central-peak mechanisms have been proposed, some of which may apply in our case: phasons and overdamped soft modes, entropy- and phonon-density fluctuations and the phenomena of coupling between these fluctuations and the soft modes, cluster and domain wall dynamics, the vast field of crystal defects, and critical scattering in the order–disorder limit which is usually not subsumed under the central-peak label. For a review see reference [26].

We can rule out most of these mechanisms and will dwell in more detail on the cluster and soliton scenario and on critical scattering. Moreover, due to the width of the spectral window (± 3 cm^{-1}), the intensity contributions of the Brillouin components also have to be taken into account. However, the variations of the sound velocities at the various phase transitions are small in BCCD [41], except at T_i. Hence, the contributions from inelastic (Brillouin) scattering to the observed anomalies are small, save for the peak at T_i.

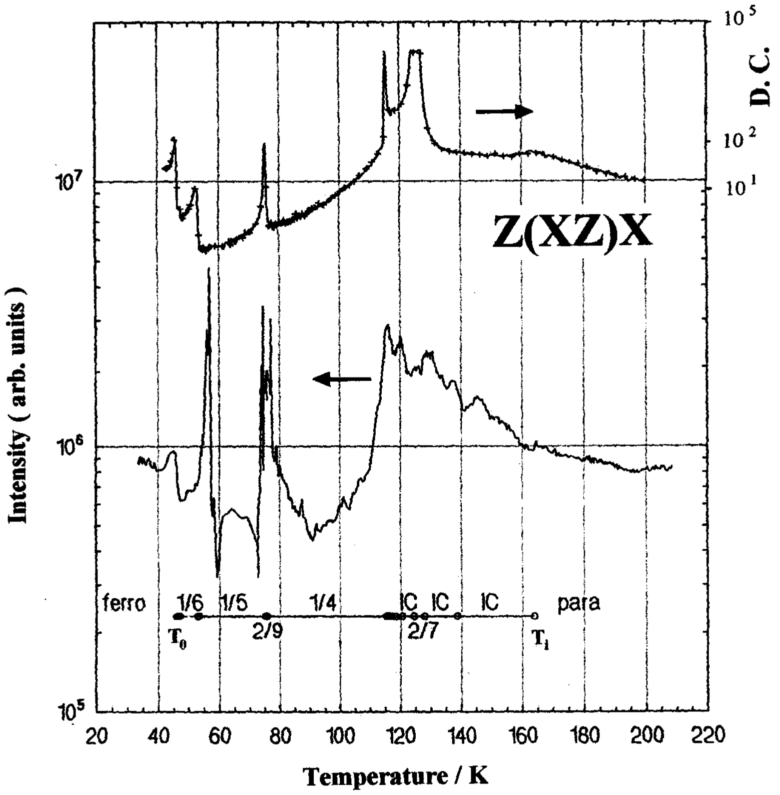

(b)

Figure 1. (Continued)

The intensity of scattering due to entropy fluctuations† [42] is governed by the temperature derivative of the refractive index, $I_S \sim (\mathrm{d}n/\mathrm{d}T)^2$ [26]. For this to become effective in BCCD, appreciable jumps of n at the phase transition temperatures are required to produce the observed peak intensity. Unfortunately, precise measurements of n or of the double refraction Δn_{ij} only exist for BCCD for the interval 100 K $\leqslant T \leqslant$ 200 K [43]. From the published plots we find at T_{L_2}: $\Delta n_{ab} = 2.0 \times 10^{-5}$, $\Delta n_{ac} = 2.7 \times 10^{-5}$, $\Delta n_{bc} < 0.5 \times 10^{-5}$. Obviously these small variations of n cannot be responsible for the large central peak at T_{L_2}. Phonon-density fluctuations produce effects in the far wings of the central peaks [26] and again will not contribute as the prime source of scattering, although the low-lying modes near 30 cm^{-1} mentioned above might produce such fluctuations.

The role of impurities is more complex [44, 45]. In BCCD the 'frozen impurity' category, according to the classification of Halperin and Varma [44], is dominant, as in most cases T_C is lowered in BCCD with increasing impurity concentration [2]. In this case the displacement field in any unit cell due to an impurity or defect is the sum of two contributions: a static part and a fluctuating part with zero mean. The two parts contribute additively to the dynamical structure factor $S(\boldsymbol{q}, \omega)$ which is monitored in a scattering experiment. It has been shown [44] that the static part produces a temperature dependence of the central-peak intensity according to

† Not to be confused with entropy fluctuations due to changes in soliton density $\bar{n}$.

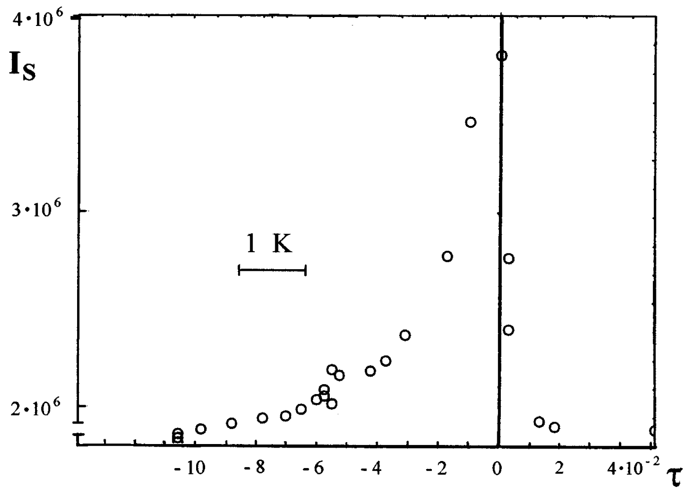

Figure 2. The intensity I_S of the central-peak anomaly at $T_0 = 46$ K $(z(yy)x)$ for BCCD; detail of figure 1(b) with an extended T-scale, and background ($\approx 1.6 \times 10^6$) subtracted; $\tau = (T - T_0)/T_0$.

$|T - T_C|^{-1}$ with the possible inclusion of logarithmic corrections in a uniaxial dipolar system. The fluctuating contribution to $S(\boldsymbol{q}, \omega)$ is proportional to the impurity-induced susceptibility χ_p. χ_p mirrors the local symmetry reduction by producing anomalies in directions of the external field which are free from such anomalies in the pure sample. Hence impurities produce central peaks with a temperature dependence essentially $\sim|T - T_C|^{-1}$ and small depolarized peaks in new directions. This does not correspond to our experimental findings. All the more, the polarization of the observed anomalies reflects the full symmetry of the unit cell, and we did not observe in the sample under study the well known shifts of transition temperatures with defect concentration and the detrimental effects of defects on the devil's staircase behaviour in BCCD [2]. On the other hand, impurity-induced dielectric susceptibility anomalies have been observed in doped crystals in directions where anomalies do not occur in the pure crystal [46]. Our conclusion is that impurities cannot be considered as the prime source of central peaks in BCCD. On the contrary, we expect that in the soliton regime the strengths of central peaks will be reduced with growing impurity concentration due to pinning of the fluctuating domain walls just as is observed for the dielectric susceptibility [2]. The true contribution of defects to the various peaks can only be characterized safely by a high-resolution study of the static scattering.

Thus, we concentrate on the effects of domain walls. The generally accepted view [47] of the essential physics of central peaks as due to cluster formation is also valid for the present system. At T_i, BCCD undergoes a phase transition of the displacive type [34]. On approaching T_i from above and with the onset of criticality [48], the growth in short-range order starts a crossover from a regime of collective displacive motions of large amplitudes to a regime where the collective behaviour is rather of the order–disorder type. For this to happen, we have to assume a double-minimum potential for the critical motions of the relevant atoms or atomic groups with a rather low central barrier. Such a crossover is then indicated by the appearance of domains or clusters of such atoms or groups with strongly correlated motions, modulated with the wavevector $\boldsymbol{q}_i$ in the case of BCCD. The average displacement of these particles within the domains is non-zero and opposite in the differently oriented clusters. The cluster sizes increase on approaching T_i or any other phase transition displaying a central peak.

The two regimes are characterized by different timescales: a single one in the displacive regime, determined by the soft high-temperature phonon, and the two timescales typical of the order–disorder regime. For the latter, the critical timescale is governed by the diffusion of the domain walls, giving rise to a central component in the dynamical response function $S(\boldsymbol{q}, \omega)$, the central peak. This response is the dynamic precursor of the static Bragg peak that appears in the low-temperature phase. The other, non-critical timescale is set by the quasi-periodic motions of small amplitudes about the positions of local equilibrium in one of the two minima, showing up as a high-frequency phonon side band in $S(\boldsymbol{q}, \omega)$, not displaying any softening in an Ising system that is strictly of order–disorder type.

For the theoretical investigation of the cluster dynamics close to a structural phase transition following this concept, two different strategies have been followed which give closely correlated results. Both approaches, an analytical study of large-amplitude, essentially anharmonic atomic motions [51–54] and a numerical study of molecular dynamics [53], start from a classical double-minimum Hamiltonian (a discrete Φ^4 system) [49]; see also [5, 40]:

$$\mathcal{H} = \sum_i \left[\left(\frac{a}{2} u_i^2 + \frac{b}{4} u_i^4 \right) + \frac{m}{2} \dot{u}_i^2 + \sum_j \frac{c_{i,j}}{2} (u_i - u_j)^2 \right]. \tag{1}$$

Here i, j indicate lattice sites, $a_i, b_i, c_{i,j}$ are temperature-independent potential coefficients, $(a < 0; b, c_{i,j} > 0)$, and $u_i, \dot{u}_i$ are displacements (translational or librational amplitudes) and velocities of particles with mass m with respect to the reference lattice; $c_{i,j}$ is the interparticle coupling constant. The two minima are separated by $y_0 = 2(|a|/b)^{1/2}$; the central potential barrier amounts to $|a|^2/4b$, which increases in BCCD under external hydrostatic pressure [2].

Analytical solutions of (1) have been obtained for a one-dimensional (1D) chain in references [49, 51, 52]; they have been extended approximatively to 2D and 3D systems and by computer simulations in [50]. The solutions of (1) decompose into two classes: (a) solutions at small amplitude f for the particle elongation $\left(f \ll (|a|/b)^{1/2}\right)$, and (b) solutions of the large-amplitude regime $\left(f \approx (|a|/b)^{1/2}\right)$. One set of solutions for class (a) describe the quasi-harmonic small-amplitude oscillations in one of the two wells, giving rise to the delocalized phonons of the system. These are the only excitations which can be detected in a spectroscopic experiment. The solutions of class (b) are of more interest in our context: these large-amplitude solutions describe non-linear excitation patterns where the elongations are constant everywhere (the particles are either in the left-hand or in the right-hand minimum), except in a small localized region (domain wall, soliton, kink) where they change sign. This solution has the form of a hyperbolic tangent, where the soliton can move freely along the modulation wavevector and the width can be estimated as $\leqslant 3$ lattice constants.

Another solution is a travelling ‘breather’ which consists of a kink and a nearby antiphase kink. This breather amplitude is zero everywhere (all particles occupy either the left-hand or the right-hand minimum), except in a small region, where the opposite well is populated [49, 51].

Particles crossing the barrier will not be encountered in a microscopic system. Instead, the particles within a domain wall are distributed statistically over their two wells, thus giving rise to the observed transition entropy and the interface roughness. Spatial and temporal correlations between solitons will grow exponentially with T approaching the transition temperatures. $S(\boldsymbol{q}, \omega)$ has been calculated and a central peak of intensity I_{cp} is obtained.

Clearly no phase transition occurs on the 1D Ising chain at $T > 0$, but in 2D and 3D systems [50], due to interchain coupling, a phase transition occurs at a finite temperature, which corresponds to T_0 in BCCD. Solitons cease to exist at high density when their width and their average distances are coming close. This might occur in BCCD at T_{L_2} with the onset of the regime of harmonic modulation and it is probably marked by the T_S-anomaly [17].

The numerical molecular dynamics calculations in 2D [53] support the previous results and the conclusions drawn. It becomes apparent also from these results that the cluster dynamics with the critical timescale, the diffusive motion of the domain walls, is one of the origins of the central peaks.

This discussion of free solitons, where $\bar{n}$ varies continuously with T, is not directly applicable to BCCD. With the entry into the c phases at T_0 the strong correlation between the solitons and an additional lock-in potential [9, 10, 12], which is not considered in (1), will fix the domain walls at certain positions of the background lattice. At best, only field-induced structural phase transitions within the soliton lattice are allowed [17], i.e. shifts of each second domain wall by one lattice constant, thus increasing the size of the polar microdomains oriented in the direction of the external field and, as a consequence, the polarization of the sample. Nevertheless, the soliton concept provides a plausible and intuitively appealing interpretation of a number of experimental observations presented here.

The interpretation of the central peak at T_0 in the single-particle order–disorder regime as due to critical scattering (compare [39]) has to consider the wavevector-dependent pseudo-spin ($S = \pm 1$) susceptibility $\chi(\boldsymbol{q}, T)_{\omega=0}$ which is proportional to the spatial Fourier transform of the pseudo-spin correlation function $\langle S_0(t = 0) S_r(0)\rangle_T$ (the susceptibility fluctuation theorem). In optical scattering the fluctuations of $\chi(\boldsymbol{r})$ and of the pseudo-spins have to be considered [37]. $\chi(\boldsymbol{r})$ is coupled to the pseudo-spin variables. The $\boldsymbol{q}$-dependence of the response function χ expresses the fact that in a light scattering experiment only Fourier components of the correlation function at the long (laser) wavelengths are observed which occur in correspondingly large clusters of correlated spins. Such clusters are found only very close to T_0 (figure 2). On the other hand, in elastic neutron scattering ($\lambda \approx 1$ Å) near T_0, the Fourier components at short wavelengths are traced, i.e. small clusters are also detected; hence the critical scattering anomaly should be much broader on the T-axis, which is in fact observed [22]. At present, we can only speculate about the type and shape of the fluctuating pseudo-spin clusters in the high-symmetry, homogeneous fe phase. Perhaps breathers or regions of correlated solitons and antisolitons with a finite correlation in all three dimensions will occur, with a distribution of S approaching the pattern of the pseudo-spin structures above T_0 in the high-symmetry phase [39]. The branch of the critical scattering above T_0 where χ decays with growing T is not fully developed because the system passes through a sequence of c $\leftrightarrow$ c$'$ phase transitions in a narrow T-interval here. It would be interesting to study these phenomena at T_0 in more detail.

Remarkably, the widths of the two anomalies at $T \approx 75$ K and $T \approx 53$ K in the $z(xz)y$ polarization are larger than at T_0, despite the fact that all of these transitions occur between almost completely ordered phases (see figure 36 in [2]). Apparently, in this case the Fourier transform of the pseudo-spin correlation function comprises long-wavelength components even far away from the transition temperatures. Such large clusters of strong correlation will occur when the regular modulation in phase δ is interrupted by a defect due to a small region ($\ll\lambda$) with the fluctuating modulation δ' of the competing phase. These considerations apply on both sides of the transition.

The asymmetry of these two anomalies is the most spectacular feature in the plot. Here the two neighbouring phases differ in soliton density, i.e. in entropy density, by $\Delta\delta = \frac{1}{20}$ ($\frac{1}{4} \leftrightarrow \frac{1}{5}$) or $\frac{1}{30}$ ($\frac{1}{5} \leftrightarrow \frac{1}{6}$). Fluctuating regions of the two bordering phases penetrate each other in the transition regions, with the corresponding correlation lengths growing or decreasing with temperature.

The asymmetry must be attributed to the interference of two coherent scattering processes in an otherwise incoherently scattering (fluctuating) system: in the standard treatment of Rayleigh light scattering [36, 37] owing to (entropy-) density fluctuations, the field-induced electric dipole moment $\boldsymbol{p}$ in an (isotropic) fluctuating region of spherical shape (radius a) is considered as the source of the scattered radiation. The excess dipole moment within the fluctuating volume element of the defective modulation is related to the dielectric constants through

$$\boldsymbol{p} = \epsilon_0 \epsilon a^3 \left(\frac{\epsilon' - \epsilon}{\epsilon' + 2\epsilon} \right) \boldsymbol{E}_0 \tag{2}$$

for $\epsilon' \approx \epsilon$, $\Delta\epsilon = \epsilon' - \epsilon$, and

$$\boldsymbol{p} \approx \epsilon_0 \frac{a^3}{3} \Delta\epsilon \, \boldsymbol{E}_0 \tag{3}$$

where ϵ is the average dielectric constant of BCCD at high frequencies in the previous c phase considered and ϵ' is the particular value in the region of the fluctuation into the new c$'$ phase with $\bar{n}'$ differing from $\bar{n}$.

In the $\delta = \frac{1}{5}$ phase the values of the ϵ-components in all three directions $i = x, y, z$ are lower than in both of the neighbouring phases (see figure 1, and the values given above). Accordingly, $\Delta\epsilon$ may have either sign; the scattered waves arising from $\boldsymbol{p}$ will interfere either constructively or destructively with elastically scattered radiation originating from other sources like static defects. The observation of interfering amplitudes with opposite phases of scattered radiation thus supports again the interpretation of the intensity anomalies as primarily due to dynamic fluctuation effects, not to a static defect-induced mechanism alone. Other sources of these asymmetric anomalies like specific absorption of light or anomalies in other background scattering phenomena (Brillouin or defect scattering, interference in the scattering amplitude from first and second sound, as discussed by Wehner and Klein [42]) can be discarded.

There is some formal resemblance of these asymmetric peaks on the temperature axis with Fano anomalies (antiresonances) of two overlapping and interacting resonant excitations on the frequency scale often observed in light scattering (see e.g. [38]). In both cases a shift of π of the relative phase occurs on crossing the phase transition temperature or the resonance frequency of the partner with the lower damping. In the Fano case, however, the interference is quantum mechanical.

With elastic neutron scattering, anomalous intensities at c $\leftrightarrow$ c$'$ phase transitions ($\delta = \frac{1}{4} \leftrightarrow \frac{1}{5}$, $\frac{1}{5} \leftrightarrow \frac{1}{6}$) in partially deuterated BCCD have been observed before [54–56]. In these investigations the complex temperature dependence of the integrated intensities $I_S(T)$ of the first-order satellites (0, 6, $\pm\delta$) at various hydrostatic pressures $p \leqslant 400$ MPa have been studied. With decreasing temperature, $I_S(T)$ displays a sequence of increasing ramps, horizontal plateaus, and steep discontinuities at the phase boundaries, in contrast to the monotonic increase on cooling often observed in other ic systems [12,57]. With growing p, the variation of $I_S(T)$ appears smoother, some peaks and plateaus being erased. At $p = 400$ MPa and beyond, the course of $I_S(T)$ is free from any anomaly and as smooth as in other ic systems. The fwhm of these anomalous peaks on the T-axis is $\approx$5 K; thus it is comparable to that of the optical peaks at $\frac{1}{4} \leftrightarrow \frac{1}{5}$, $\frac{1}{5} \leftrightarrow \frac{1}{6}$; the asymmetry of the optical scattering is not displayed here. This effect was tentatively attributed [54] to the hypothetical existence of a second order parameter of symmetry Λ_2 in BCCD below 115 K and its static coupling to the primary order parameter of symmetry Λ_3, the amplitude of modulation [3]. This order parameter Λ_2 would infer a monoclinic deformation of BCCD at low temperatures, which is not observed. It is tempting, however, to interpret these neutron results together with the Rayleigh scattering again as due to fluctuations of the pseudo-spins at the transitions, and the second order parameter invoked as the scalar soliton density $\bar{n}$. The intensity transfer from the Bragg peaks to the first-order satellites may be understood using the well known intensity relations for the satellites [1, 57].

If we compare these satellite peaks in neutron scattering with the optical peak at T_{L_2} (ic $\leftrightarrow$ c) however, a strong discrepancy in shape is encountered due to the asymmetry of the optical anomaly. Here the broad peak in the optical scattering contrasts with the symmetric and narrow neutron peaks, displaying a behaviour opposite to that of the peak at T_0 in both neutron [22] and light scattering. In consequence, the long-wavelength pseudo-spin fluctuations at $T > T_{L_2}$ are found to be larger than the short-wavelength Fourier components of the correlation observed with neutrons. Such a behaviour is characteristic for a roughening transition [58] of the domain walls expected at the transition from square-wave to harmonic modulation at T_{L_2}. At this roughening transition, which is usually rather diffuse, the interfaces in their original positions are lost due to the formation of large 2D clusters attached to the previous interface and displaying the same pseudo-spin orientation as in the adjacent layer on the left or right, respectively. More such clusters are stacked upon each other with increasing T. The width of the interface, i.e. the mean square displacement of a given point on the surface, diverges at the roughening transition, i.e. the interfaces themselves wander arbitrarily far from the original reference plane [17]. The roughness of the interfaces is often discussed in the discrete Gaussian model [58, 59], in which the energies of interaction between nearest-neighbour pseudo-spin chains varies quadratically with the length differences between identically oriented sections, or the excess free energy of the interface depends quadratically on the two-dimensional wavevector of the surface roughness. Stated differently, at the roughening transition only long-wavelength fluctuations in the position of the interface are encountered while short wavelengths are irrelevant because of the high energies involved, characteristic for surface tension. A roughening transition of domain walls is also considered to occur in Rb_2ZnCl_4 at $T^* \approx 160$ K ($<T_L$) [60]. Below T^* the coercive field starts to increase in this material as was also observed in BCCD below T_S [17].

The disappearance of the anomalous neutron scattering at elevated pressure corresponds to the existence of the diffuse phase transition in BCCD at the anomaly T_S [17], which obviously separates the regions of square-wave and harmonic modulation. The pressure dependence observed for the anomalies in elastic neutron scattering $I_S(T, p)$ [54–56] fully corresponds to the behaviour of $T_S(p)$ [17]. A similar decay of central-peak intensity can also be anticipated for optical scattering in the (p, T) region above T_S.

Most of our arguments and interpretations given above are based on the assumption that strong anharmonicity of the lattice potential, as expressed by equation (1), is effective in BCCD for the modes triggering the phase transitions. We have to realize that the mechanism for the transition n $\leftrightarrow$ ic at T_i has already been successfully interpreted in a quasi-harmonic semi-microscopic model [34], based on extensive investigations of inelastic scattering of neutrons and on the hypothesis that the modes involved are in-phase and out-of-phase librations of the betaine and the inorganic pseudo-octahedral Ca complexes in the unit cell, both coupled to the translations of the LA branch propagating in the z-direction. The present results require in addition that these modes occur with large amplitudes at both T_i and T_{L_2}. This assumption is in fact reasonable as these modes show very low frequencies (<25 cm^{-1}) at these temperatures and large thermal occupation factors:

$$n' = \left(\exp\left(\frac{\hbar\omega}{kT}\right) - 1\right)^{-1}$$

ranging from 3 to 18. Even at $T = 35$ K in the fe phase the lowest modes at 30 cm^{-1} [40] are well populated ($n' = 0.64$) and display a high density of phonon states. Beyond that, both low-lying librational modes display a $\boldsymbol{q}$-dependence [40], which is almost free of dispersion and indicates strongly localized excitations. Hence the conditions for the existence of anharmonic excitations in BCCD are well met.

4. Conclusions

We have investigated the temperature-dependent quasi-elastic light scattering of nominally pure BCCD in two polarization directions.

The shapes of the observed anomalies mirror the two regimes of the modulated phases of BCCD: the region of harmonic modulation is characterized by broad (≈20 K fwhm) maxima; the region of square-wave modulation is characterized by narrow, asymmetric peaks ($\leqslant$5 K fwhm). At ambient pressure, the two regimes are separated by the T_S-anomaly.

All anomalies have been interpreted on the hypothesis that they are primarily intrinsic properties, i.e. not due to lattice defects or to impurities. On this basis the peaks occurring at $T > T_0$ can be attributed essentially to the softening of the well known optical modes near T_i and to low-lying Raman-active optical phonons near $T = 130$ K, while at $T < T_S$ the intensity anomalies display the characteristic features of critical scattering due to the order–disorder type of the c $\leftrightarrow$ c$'$ transitions in this Ising pseudo-spin system.

While all features observed by us in the spectra support this hypothesis, for a final assignment additional and more exact data will be required. Most importantly, precise experiments at high spectral resolution, perhaps with variation of external parameters, e.g. pressure or electric field, will be essential to determine the temperature-dependent widths of the central peaks and to discriminate reliably between the various mechanisms contributing to their intensity. Detailed investigation of the transition at T_0 appears to be especially promising.

BCCD can be characterized by saying that this material displays not only a large number of modulated phases, but also a large variety of unconventional phase transitions (of both the displacive and the order–disorder type) marked by central peaks of considerable complexity, which are conveying some important details about these transitions.

Acknowledgments

The authors are indebted to Dr O Hernandez, University of Lille, and to the referees of this paper for critical and stimulating remarks.

References

[1] Cummins H Z 1990 *Phys. Rep.* **185** 211
[2] Schaack G and le Maire M 1998 *Ferroelectrics* **208** 1
[3] Pérez-Mato J M 1988 *Solid State Commun.* **67** 1145
[4] Unruh H-G, Hero F and Dvořák V 1989 *Solid State Commun.* **70** 403
[5] Neubert B, Pleimling M and Siems R 1998 *Ferroelectrics* **208** 141
[6] Tentrup Th and Siems R 1990 *Ferroelectrics* **105** 813
[7] Neubert B, Pleimling M, Tentrup Th and Siems R 1994 *Ferroelectrics* **155** 359
[8] Kappler C and Walker M B 1993 *Phys. Rev.* B **48** 5902
[9] Ribeiro J L, Tolédano J C, Chaves M R, Almeida A, Müser H E, Albers J and Klöpperpieper A 1990 *Phys. Rev.* B **41** 2343
[10] Sannikov D G and Schaack G 1998 *J. Phys.: Condens. Matter* **10** 1803
[11] Cowley R A and Bruce A D 1977 *J. Phys. C: Solid State Phys.* **11** 3577
[12] Tolédano J-C and Tolédano P 1987 *The Landau Theory of Phase Transitions* (Singapore: World Scientific)
Kociński J 1990 *Commensurate and Incommensurate Phase Transitions* (Amsterdam: Elsevier)
[13] Ao R, Schaack G, Schmitt M and Zöller M 1989 *Phys. Rev. Lett.* **62** 183
[14] Freitag O and Unruh H-G 1990 *Ferroelectrics* **105** 357

Freitag O 1992 *PhD Thesis* University of Saarbrücken

[15] Hernandez O, Quilichini M, Cousson A, Paulus W, Kiat J-M, Goukassov A, Ezpeleta J M, Zúñiga F J, Pérez-Mato J M, Dušek M and Petříček V 1998 *Proc. Int. Conf. on Aperiodic Crystals (Aperiodic '97)* ed M de Boissieu, J-L Verger-Gaugry and R Currat (Singapore: World Scientific) p 365

Hernandez O, Kiat J-M, Cousson A, Paulus W, Ezpeleta J M and Zúñiga F J 1999 *Acta Crystallogr.* C **55** 1463

Hernandez O, Quilichini M, Pérez-Mato J M, Zúñiga F J, Dušek M, Kiat J-M and Ezpeleta J M 1999 *Phys. Rev.* B **60** 7025

[16] Ezpeleta J M, Zúñiga F J, Pérez-Mato J M, Paciorek W and Breczewski T 1992 *Acta Crystallogr.* B **48** 261

[17] le Maire M, Straub R and Schaack G 1997 *Phys. Rev.* B **56** 134

[18] The widths of the well known 180° domain walls in the fe phase are larger by approximately one order of magnitude (e.g. ≈12 nm in TGS); see

Szcześniak L, Hilczer B and Meyer K-P 1995 *Ferroelectrics* **172** 227

[19] Igartua J M, Ruiz-Larrea I, Breczewski T and López-Echarri A 1994 *Phase Transitions* **50** 227

Brill W, Gmelin E and Ehses K H 1990 *Ferroelectrics* **103** 25

[20] Hlinka J and Ishibashi Y 1998 *J. Phys. Soc. Japan* **67** 912

[21] Bak P 1981 *Solitons and Condensed Matter Physics (Springer Series in Solid-State Sciences vol 8)* ed A R Bishop and T Schneider (Berlin: Springer) p 216

[22] Hernandez O, Quilichini M and Schaack G 2000 to be published

[23] Quilichini M *et al* 1999 private communication

[24] le Maire M and Schaack G 1995 *Ferroelectrics* **172** 187

[25] Parlinski K, Dénoyer F and Eckold G 1991 *Phys. Rev.* B **43** 8411

[26] Fleury P A and Lyons K B 1983 *Light Scattering near Phase Transitions (Modern Problems in Condensed Matter Sciences vol 5)* ed H Z Cummins and A P Levanyuk (Amsterdam: North-Holland) p 449

[27] Rother H J, Albers J and Klöpperpieper A 1984 *Ferroelectrics* **54** 107

[28] Ao R and Schaack G 1988 *Ferroelectrics* **80** 105

[29] Kamba S, Petzelt J, Dvořák V, Goncharov Yu G, Volkov A A and Kozlov G V 1993 *J. Phys.: Condens. Matter* **5** 4401

[30] Neubert B, Pleimling M and Siems R 1998 *J. Phys.: Condens. Matter* **10** 6883

[31] Neubert B and Pleimling M 1998 *J. Phys. Soc. Japan* **67** 3324

Hlinka J and Ishibashi Y 1998 *J. Phys. Soc. Japan* **67** 3326

[32] Ao R and Schaack G 1988 *Indian J. Pure Appl. Phys.* **26** 124

[33] Wilhelm H and Unruh H-G 1991 *Z. Kristallogr.* **195** 75

[34] Hlinka J, Quilichini M, Currat R and Legrand J F 1996 *J. Phys.: Condens. Matter* **8** 8207

Hlinka J, Quilichini M, Currat R and Legrand J F 1996 *J. Phys.: Condens. Matter* **8** 8221

Hlinka J, Quilichini M, Currat R and Legrand J F 1997 *J. Phys.: Condens. Matter* **9** 1461

[35] Blinc R, Prelovšek P, Rutar V and Žumer S 1986 *Incommensurate Phases in Dielectrics (Fundamentals) (Modern Problems in Condensed Matter Sciences vol 14.1)* ed R Blinc and A P Levanyuk (Amsterdam: North-Holland) p 143

Axe J D, Iizumi M and Shirane G 1986 *Incommensurate Phases in Dielectrics (Materials) (Modern Problems in Condensed Matter Sciences vol 14.2)* ed R Blinc and A P Levanyuk (Amsterdam: North-Holland) p 1

[36] Kerker M 1969 *The Scattering of Light* (New York: Academic)

[37] Chu B 1974 *Laser Light Scattering* (New York: Academic)

[38] Wehner R K and Steigmeier E F 1975 *RCA Rev.* **36** 70

[39] Als-Nielsen J 1976 *Phase Transitions and Critical Phenomena* vol 5a, ed C Domb and M S Green (London: Academic) p 87

[40] Hlinka J, Hernandez O, Quilichini M and Currat R 1996 *Ferroelectrics* **185** 221

[41] Haussühl S, Liedtke J, Albers J and Klöpperpieper A 1988 *Z. Phys.* B **70** 219

Kityk A V, Soprunyuk V P, Vlokh O G, Sveleba S A and Czapla Z 1993 *J. Phys.: Condens. Matter* **5** 7415

[42] Wehner R K and Klein R 1972 *Physica* **62** 161

[43] Kroupa J, Albers J and Ivanov N R 1990 *Ferroelectrics* **105** 345

[44] Halperin B I and Varma C M 1976 *Phys. Rev.* B **14** 4030

[45] Levanyuk A P and Sigov A S 1988 *Defects and Structural Phase Transitions* (New York: Gordon and Breach)

[46] Ao R, Lingg G, Schaack G and Zöller M 1990 *Ferroelectrics* **105** 391

[47] Bruce A D 1981 *Solitons and Condensed Matter Physics (Springer Series in Solid-State Sciences vol 8)* ed A R Bishop and T Schneider (Berlin: Springer) p 116

[48] Holzer K P, Petersson J, Schüssler D, Walisch R, Häcker U and Michel D 1993 *Phys. Rev. Lett.* **71** 89

Häcker U, Petersson J, Walisch R and Michel D 1996 *Z. Phys.* B **100** 441

[49] Krumhansl J A and Schrieffer J R 1975 *Phys. Rev.* B **11** 3535

[50] Koehler T R, Bishop A R, Krumhansl J A and Schrieffer J R 1975 *Solid State Commun.* **17** 1515
Bishop A R and Krumhansl J A 1975 *Phys. Rev.* B **12** 2824

[51] Varma C M 1976 *Phys. Rev.* B **14** 244

[52] Aubry S 1975 *J. Chem. Phys.* **62** 3217

[53] Schneider T and Stoll E 1976 *Phys. Rev.* B **13** 1216
Schneider T and Stoll E 1981 *Solitons and Condensed Matter Physics (Springer Series in Solid-State Sciences vol 8)* ed A R Bishop and T Schneider (Berlin: Springer) p 135

[54] Almeida A, Chaves M R, Kiat J K, Schneck J, Schwarz W, Tolédano J-C, Ribeiro J L, Klöpperpieper A, Müser H E and Albers J 1992 *Phys. Rev.* B **45** 9576

[55] Chaves M R, Almeida A, Tolédano J-C, Schneck J, Kiat J M, Schwarz W, Ribeiro J L, Klöpperpieper A, Albers J and Müser H E 1993 *Phys. Rev.* B **48** 13 318

[56] Chaves M R, Almeida A, Tolédano J-C, Schneck J, Glass R, Schwarz W, Ribeiro J L, Klöpperpieper A and Albers J 1995 *Phys. Status Solidi* b **189** 97

[57] Axe J D, Iizumi M and Shirane G 1986 *Incommensurate Phases in Dielectrics (Materials) (Modern Problems in Condensed Matter Sciences vol 14.2)* ed R Blinc and A P Levanyuk (Amsterdam: North-Holland) p 1

[58] Weeks J D 1979 *Ordering in Strongly Fluctuating Condensed Matter Systems (NATO ASI Series B, vol 50)* ed T Riste (New York: Plenum) p 293

[59] Lajzerowicz J 1980 *Ferroelectrics* **24** 179

[60] Hauke T, Mueller V, Beige H and Fousek J 1998 *Phys. Rev.* B **57** 10 424